

Langevin Dynamics Deciphers the Motility Pattern of Swimming Parasites

Vasily Zaburdaev,^{1,2} Sravanti Uppaluri,³ Thomas Pfohl,^{4,3} Markus Engstler,⁵ Rudolf Friedrich,⁶ and Holger Stark²

¹*School of Engineering and Applied Science, Harvard University, Cambridge, Massachusetts 02138, USA*

²*Institute of Theoretical Physics, Technical University of Berlin, D-10623 Berlin, Germany*

³*Max-Planck-Institute for Dynamics and Self-Organization, Göttingen, D-37073, Germany*

⁴*Department of Chemistry, University of Basel, Basel, CH-4056, Switzerland*

⁵*Biocenter, University of Würzburg, Würzburg, D-97074, Germany*

⁶*Institute of Theoretical Physics, University of Münster, Münster, D-48149 Germany*

(Received 29 September 2010; published 20 May 2011)

The parasite African trypanosome swims in the bloodstream of mammals and causes the highly dangerous human sleeping sickness. Cell motility is essential for the parasite's survival within the mammalian host. We present an analysis of the random-walk pattern of a swimming trypanosome. From experimental time-autocorrelation functions for the direction of motion we identify two relaxation times that differ by an order of magnitude. They originate from the rapid deformations of the cell body and a slower rotational diffusion of the average swimming direction. Velocity fluctuations are athermal and increase for faster cells whose trajectories are also straighter. We demonstrate that such a complex dynamics is captured by two decoupled Langevin equations that decipher the complex trajectory pattern by referring it to the microscopic details of cell behavior.

DOI: [10.1103/PhysRevLett.106.208103](https://doi.org/10.1103/PhysRevLett.106.208103)

PACS numbers: 87.17.Jj, 05.10.Gg, 05.40.-a, 87.10.Mn

Introduction.—The motility of cells in nature is of crucial importance to several processes of their life cycle. Wound healing, tumor growth, fertilization, infection spreading—all these processes only function when the corresponding agents are motile [1]. Whatever these agents are, cells or bacteria, they are present in multitudes and can move collectively in complex and heterogeneous environments, such as tissue or blood vessels. Observing the trajectory of a single cell in a well-controlled environment allows us to focus exclusively on its motility.

In this Letter we aim to analyze the motility of the African trypanosome (*Trypanosoma brucei brucei*)—a parasite that swims in the blood stream and infects mammals often causing fatal diseases [2–8]. Unique features of trypanosome motility are already visible on the microscopic level. The trypanosome's elongated cell body has the shape of a spindle, to which a single flagellum is attached. The beating flagellum causes the whole body to deform strongly which results in a complex swimming pattern [5,6] (see supplemental material [9]: movie 1). On the millimeter scale, a trajectory of a swimming trypanosome looks like a classical random walk. Previous work in statistical physics offers a wealth of models to explain random-walk trajectories and they are successfully used to analyze the motility patterns of various microorganisms. For example, random-walk models describe classical and anomalous diffusion of cells and bacteria [10]; different types of Langevin equations are also employed [11,12]. However, all of these models appear to be too simplistic to be applied to swimming trypanosomes.

The most striking feature of the experimental data is the presence of two characteristic relaxation times in the

velocity autocorrelation function that differ by more than an order of magnitude. Velocity fluctuations reveal another level of complexity—faster organisms exhibit larger fluctuations; however, their trajectories are more straight or persistent. In the following we suggest a theoretical model which explains all these intriguing features and quantitatively describes the large-scale motion of the trypanosome but also takes into account its distinct body distortions.

Experimental setup.—The bloodstream form of trypanosomes is found in blood vessels densely populated by red blood cells where they are subjected to strong shear stresses [2,5,6]. In order to first concentrate and understand the motility of a trypanosome itself, we have chosen a minimal, quasi-two-dimensional setup in which the motion of cells was confined between two glass plates separated by a distance of 10 μm . A suspension of trypanosomes in fresh HMI9 medium (viscosity 1 cP) [13] was monitored at room temperature with a 10 \times objective (0.64 μm spatial resolution). The confinement was required to maintain the trypanosomes within the focal plane and allowed us to continuously monitor single cells well separated from others with a frame rate of 1 Hz. We recorded cell trajectories for up to 30 min from which we realized that the average speed of the cells slowly decreased on a time scale of about 20 min much larger than the characteristic time scales of the system (for further discussion of the setup see the supplemental material [9]). In order to minimize the influence of this behavior on our data analysis, we ultimately used the tracking data of the first 150 seconds from 41 trajectories.

A typical trajectory of the center of mass of the trypanosome is shown in Fig. 1 (see also supplemental material

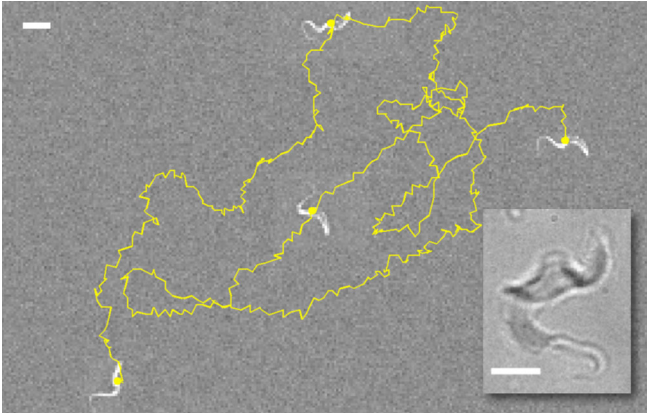


FIG. 1 (color online). A typical trajectory of a swimming trypanosome (scale bar is $10 \mu\text{m}$). Note a persistence in straight motion perturbed by strong fluctuations. The inset shows the snapshot of a *Trypanosoma brucei brucei* (scale bar is $5 \mu\text{m}$).

[9]: movie 2). On the scale of microns, we see a “noisy” zigzag-like motion generated by the intense and rapid cell-body deformations. They result from a distortional wave [6] that runs from the thinner tail to the thicker end of the elongated cell body. It creates the nonreciprocal body deformation necessary for locomotion at low Reynolds numbers [14]. The wave produces large amplitude oscillations of the tail, similar to a recently constructed microswimmer [15], which results in the observed zigzag motion. Then, on a larger scale the trypanosome follows a smoother path which exhibits some persistence in its swimming direction.

Experimental results.—We start our analysis with the time series of the trypanosomes’ center of mass velocity defined for each time step t_i as

$$\mathbf{v}(t_i) = [\mathbf{r}(t_i + \delta t) - \mathbf{r}(t_i)]/\delta t. \quad (1)$$

Clearly the time series depend on the choice of δt . For now we set $\delta t = 2 \text{ s}$ and comment on this choice later. We first analyze the velocity autocorrelation function by dividing it into two parts—temporal correlations in the speed $|\mathbf{v}|$ and in the direction of motion $\mathbf{v}/|\mathbf{v}|$. Surprisingly, the direction of motion exhibits two characteristic relaxation times that differ by an order of magnitude (see graph of C_θ in Fig. 2). The short time is less than 1 s and the long time is about 10 s. However, in the speed correlations only the shorter relaxation time is visible (see graph of $C_{|\mathbf{v}|}$ in Fig. 2). We determined and confirmed the short correlation time using additionally recorded high-resolution data (see the inset of Fig. 2). Its value of 0.12 s obviously gives the decay time for correlations in the irregular oscillations of the rapid cell-body motion. This time corresponds to a few oscillations and is consistent with the reported flagellum beating period of 50 ms [6]. Having clarified the existence and origin of the short relaxation time, we will concentrate in the following on our main data set. These data are sufficient for developing a stochastic model for the large-scale

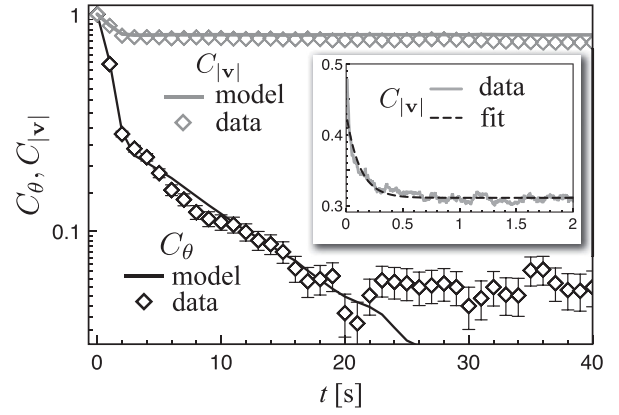


FIG. 2. Velocity autocorrelation function: angular part $C_\theta = \frac{\mathbf{e}(t_0 + t) \cdot \mathbf{e}(t_0)}{|\mathbf{e}(t_0)|^2}$ with $\mathbf{e}(t_0) = \mathbf{v}(t_0)/|\mathbf{v}(t_0)|$ and speed correlations $C_{|\mathbf{v}|} = \frac{|\mathbf{v}(t_0 + t)| |\mathbf{v}(t_0)|}{|\mathbf{v}(t_0)|^2}$. Symbols and solid lines represent data from experiments and simulations, respectively. Averaging is performed over all trajectories and over the reference time t_0 . Inset: $C_{|\mathbf{v}|}$ determined from data with high temporal resolution of 10^{-3} s . After an initial decay to ~ 0.4 due to the tracking algorithm, an exponential with correlation time 0.12 s can be fitted (dashed line).

motion of the trypanosome based on the conclusion that speed and direction of motion of trypanosomes are decoupled on time scales exceeding 1 s [16].

The distribution of speed values for all trajectories exhibits a broad non-Gaussian profile (see Fig. 3). Non-Gaussian velocity distributions have been reported and explained for other types of cells and microorganisms [11,12,17]. In our case the reason for the broad distribution is rather natural and also mentioned in literature (see, e.g., Ref. [18]): intrinsically, the cells are not identical and each trypanosome trajectory can be characterized by its mean square velocity $\langle \mathbf{v}^2 \rangle$, where $\langle \dots \rangle$ means average over one trajectory. The distribution $R(\langle \mathbf{v}^2 \rangle^{1/2})$ characterizes our set of trajectories. It is itself quite broad (see inset in Fig. 3)

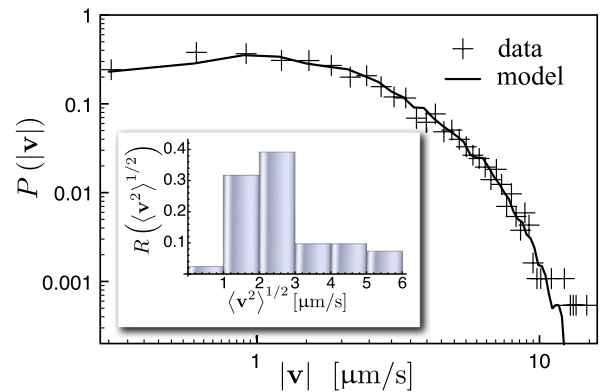


FIG. 3 (color online). Distribution of speed values $P(|\mathbf{v}|)$ for all trajectories. The histogram of the inset illustrates how the trypanosome’s mean velocity varies from cell to cell by showing the distribution R for the root mean square velocity $\langle \mathbf{v}^2 \rangle^{1/2}$ calculated for each trajectory.

and results in the broad velocity distribution for the ensemble of cells.

Besides the distribution of mean values, more information about the ensemble of trajectories is obtained from fluctuations around these mean values. For each trajectory we calculate the standard deviation of velocity squared, $\delta\mathbf{v}^2 = \langle (\mathbf{v}^2 - \langle \mathbf{v}^2 \rangle)^2 \rangle^{1/2}$, and the average directional ‘‘persistence’’ $\langle \cos \delta\theta \rangle = \langle \mathbf{v}(t + \delta t) \cdot \mathbf{v}(t) / [|\mathbf{v}(t + \delta t)| |\mathbf{v}(t)|] \rangle$ ($\delta t = 2$ s), and then check how they depend on the trajectory’s mean square velocity. Faster trypanosomes display larger velocity fluctuations $\delta\mathbf{v}^2$ as the approximately quadratic dependence on $\langle \mathbf{v}^2 \rangle^{1/2}$ shows, but their trajectories are more straight, since consecutive velocity directions are more aligned (see Fig. 4). This remarkable fact indicates that the increasing speed makes the cells more persistent.

Theoretical model.—We now formulate a model which accounts for all of the aforementioned observations. The body deformations of the trypanosome on a time scale of less than 1 s are the primary source of fluctuations. In addition, correlations of the average swimming direction decay much slower. To capture this behavior, we split the velocity of the trypanosome into two parts: $\mathbf{v} = \mathbf{w} + \mathbf{u}$.

The fast velocity fluctuations are described by \mathbf{w} and the component $\mathbf{u} = u_0(\cos\varphi, \sin\varphi)$ with the constant swimming speed u_0 slowly changes its direction through the polar angle φ . We describe the time evolution of the two dynamic variables, \mathbf{w} and φ , with the help of Langevin equations.

The polar angle φ diffuses on the unit circle and, therefore, obeys $\dot{\varphi} = g_\varphi \eta(t)$. Here $\eta(t)$ is the standard delta-correlated additive white noise with zero mean and variance $\langle \eta(t)\eta(t') \rangle = \delta(t - t')$. The noise amplitude g_φ determines the longest correlation time $\tau_\varphi = 2/g_\varphi^2 \sim 10$ s visible in Fig. 2. Note that this value clearly indicates that

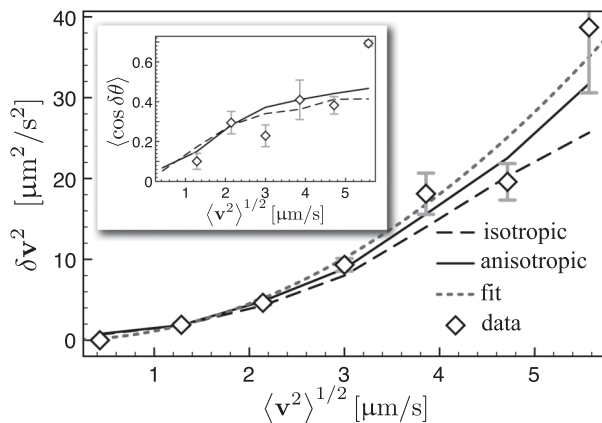


FIG. 4. Velocity fluctuations $\delta\mathbf{v}^2$ as a function of the root mean square velocity $\langle \mathbf{v}^2 \rangle^{1/2}$ of an individual cell. Experimental data are compared with simulated data from a model with isotropic (dashed line) and anisotropic noise (solid line). The gray dotted line shows a quadratic fit to the experimental data. Inset: directional persistence of a trajectory grows with the root mean square velocity of a single cell.

the rotational diffusion of the average swimming direction is a result of active rather than thermal motion of the trypanosome. When we estimate the corresponding *thermal* relaxation time τ_{th} at room temperature in water by assuming that the trypanosome is a hard rod of length $L = 20 \mu\text{m}$ and diameter $d = 2 \mu\text{m}$, we arrive at $\tau_{\text{th}} \approx 1000$ s, much larger than τ_φ .

The fast velocity fluctuations \mathbf{w} are described by a standard Langevin equation [19]:

$$\dot{\mathbf{w}} = -\mathbf{w}/\tau_w + g_w \boldsymbol{\xi}(t)/\sqrt{\tau_w}, \quad (2)$$

where $\boldsymbol{\xi}(t) = (\xi_1, \xi_2)$ is a two-dimensional vector with independent white noise components, $\langle \xi_i(t)\xi_j(t') \rangle = \delta_{ij}\delta(t - t')$, and g_w is the strength of noise. Our experimental data also show that faster cells exhibit larger velocity fluctuations. Therefore, we assume that g_w is a linear function in the cell’s average speed u_0 : $g_w(u_0) = g_0 + \alpha u_0$. Qualitatively we understand this behavior. The athermal noise generates the body distortions which ultimately propel the trypanosome. Now, if the trypanosome swims faster, the friction with the solvent increases and, therefore, the stochastic force has to increase. With recorded swimming speeds $\approx 15 \mu\text{m/s}$, the trypanosome is a low Reynolds number swimmer ($\text{Re} < 10^{-4}$) where inertia is completely negligible [14]. However, Langevin Eq. (2) conventionally describes the thermal diffusion of a Brownian particle with inertia. In our case, the inertial term is due to the active cell motion and Eq. (2) provides the short relaxation time τ_w in the trypanosome’s velocity correlations.

The speed u_0 characterizes a single trypanosome. For each trajectory $\langle \mathbf{v}^2 \rangle = u_0^2 + \langle \mathbf{w}^2 \rangle$, where $\langle \mathbf{w}^2 \rangle = (g_0 + \alpha u_0)^2$, which allows us to solve for u_0 for each value of $\langle \mathbf{v}^2 \rangle$. However, the time step δt used in Eq. (1) for calculating velocity from experimental data, is larger than the short relaxation time τ_w in Eq. (2). Consequently, the experimental value $\langle \mathbf{w}^2 \rangle_{\text{exp}}$ is smaller than the ideal or instantaneous value $\langle \mathbf{w}^2 \rangle = (g_0 + \alpha u_0)^2$ predicted by theory. We are able to link both values in the following relation (see supplemental material for derivation [9]) [20]:

$$\langle \mathbf{v}^2 \rangle_{\text{exp}} = u_0^2 + \langle \mathbf{w}^2 \rangle \frac{2\tau_w}{\delta t} \left(1 - \frac{\tau_w}{\delta t} \left[1 - e^{-\delta t/\tau_w} \right] \right). \quad (3)$$

It recovers the ideal relation in the limit $\delta t \ll \tau_w$. We use Eq. (3) to determine the distribution of u_0 from the experimental $R(\langle \mathbf{v}^2 \rangle^{1/2})$. To complete our model, we take into account the aging of the cells due to illumination by introducing exponential decay laws $u_0(t) := u_0 e^{-t/T}$ and $g_w(t) := g_w e^{-t/T}$ with $T = 1100$ s.

Theoretical modeling vs experiment.—Based on our model, we use computer simulations [21] to generate numerical data for the velocity time series. By finding the best match [20] between the numerical and experimental results for the autocorrelation functions, velocity distribution, and the amplitude of velocity fluctuations, we

determine the four unknown parameters of our model: the noise amplitudes g_φ and $g_w = g_0 + \alpha u_0$, and the fast relaxation time τ_w . A successful model should not depend on the choice of the time step δt used in the definition of velocity (1). Indeed, we checked that simulated and experimental data could be matched with the same parameters for various time steps $\delta t = 1, 2, \text{ and } 3 \text{ s}$.

The agreement between simulations and experiments is excellent, as documented in Figs. 2 and 3. The dashed lines in Fig. 4 of our current model already indicate that fluctuations δv^2 grow with increasing $\langle v^2 \rangle$ and faster cells have straighter trajectories. The latter makes sense since for increasing mean velocity u_0 the average swimming direction \mathbf{u}/u_0 is less disturbed by the fast fluctuating component \mathbf{w} .

To further advance the model, we introduce anisotropic noise in Langevin Eq. (2) by distinguishing between the respective noise components parallel and perpendicular to the average swimming direction \mathbf{u} , $g_{\parallel} = g_0 + \alpha u_0$ and $g_{\perp} = g_0 + \alpha \gamma u_0$. The coefficient γ characterizes the anisotropy of noise. The friction coefficient perpendicular to the body axis of the trypanosome is larger than the one along its elongated cell body. Therefore, we expect fluctuations generated by g_{\perp} orthogonal to the body to be weaker, meaning that $\gamma \in [0, 1]$. Indeed, both fits in Fig. 4 are improved by the anisotropic model.

The fit parameters of our model assume the following values: $\tau_w = 0.3 \text{ s}$ and $\tau_\varphi = 2/g_\varphi^2 = 11.3 \text{ s}$; for the isotropic noise, $g_0 = 1.5 \mu\text{m/s}$ and $\alpha = 1.8$, while for the anisotropic noise, $g_0 = 1.8 \mu\text{m/s}$, $\alpha = 1.9$, and $\gamma = 0.45$ indicates a pronounced anisotropy. Note that our model is not only consistent with experimental data, but also provides a prediction for the short relaxation time $\tau_w = 0.3 \text{ s}$, beyond the chosen experimental resolution of 1 s and in good agreement with our additional measurements.

As already stated, the tail of the cell body performs irregular oscillations with angular amplitude $\delta\varphi$ around the average swimming direction \mathbf{u} . Correlations in the oscillations decay within $\tau_w = 0.3 \text{ s}$ and \mathbf{u} performs an angular random-walk step $\delta\varphi$ during τ_w . Finally, temporal correlations in \mathbf{u} vanish after time t_φ meaning $\pi^2 \simeq \delta\varphi^2 t_\varphi / \tau_w$. This gives a reasonable estimate $\delta\varphi \simeq \pi/6$ and links t_φ to the rapid cell motion.

Conclusions.—We modeled the trypanosome's swimming path using two decoupled Langevin equations for the average swimming direction and the rapid fluctuations in velocity consistent with experimental observations. The stochastic forces involved are athermal and a result of the actively moving trypanosome. Properties of individual cells vary strongly, with faster cells having larger velocity fluctuations and straighter trajectories. The second observation motivated an anisotropic extension of our model with stronger velocity fluctuations along the swimming direction that improved the modeling. In this Letter

we demonstrated how the variability of properties in an ensemble of cells and also finite time resolution of experimental data can be treated. These are typical features of any experiment with microorganisms. Therefore, the model and analysis presented in this Letter will be useful for any study that investigates the swimming strategies of microorganisms by monitoring their stochastic trajectories.

We thank N. Heddergott, E. Stellamanns, S. Herminghaus, and J. Nagler for helpful discussions. Our research was supported through grants of Deutsche Forschungsgemeinschaft within the priority program SPP1207 (M.E., T.P., H.S., S.U.), scholarship ZA593/2-1 (V.Z.), and research training group GRK1558 (H.S., V.Z.).

-
- [1] D. A. Lauffenburger and A. F. Horwitz, *Cell* **84**, 359 (1996); K. F. Jarrell and M. J. McBride, *Nat. Rev. Microbiol.* **6**, 466 (2008); U. F. Greber and M. Way, *Cell* **124**, 741 (2006).
 - [2] M. Engstler *et al.*, *Cell* **131**, 505 (2007).
 - [3] J. A. Frearson *et al.*, *Nature (London)* **464**, 728 (2010).
 - [4] G. A. M. Cross, *Nature (London)* **464**, 689 (2010).
 - [5] K. S. Ralston *et al.*, *Annu. Rev. Microbiol.* **63**, 335 (2009).
 - [6] J. A. Rodríguez *et al.*, *Proc. Natl. Acad. Sci. U.S.A.* **106**, 19322 (2009).
 - [7] C. Gadelha, B. Wickstead, and K. Gull, *Cell Motil. Cytoskeleton* **64**, 629 (2007).
 - [8] R. Broadhead *et al.*, *Nature (London)* **440**, 224 (2006).
 - [9] See supplemental material at <http://link.aps.org/supplemental/10.1103/PhysRevLett.106.208103> for movies and technical details.
 - [10] H. C. Berg, *Random Walks in Biology* (Princeton University, Princeton, NJ, 1993) p. 75; P. Dieterich *et al.*, *Proc. Natl. Acad. Sci. U.S.A.* **105**, 459 (2008); R. Metzler and J. Klafter, *Phys. Rep.* **339**, 1 (2000).
 - [11] D. Selmeczi *et al.*, *Eur. Phys. J. Special Topics* **157**, 1 (2008).
 - [12] L. Li, S. F. Norrelykke, and E. C. Cox, *PLoS ONE* **3**, e2093 (2008).
 - [13] H. Hirumi and K. Hirumi, *Journal of Parasitology* **75**, 985 (1989).
 - [14] E. M. Purcell, *Am. J. Phys.* **45**, 3 (1977); E. Lauga and T. R. Powers, *Rep. Prog. Phys.* **72**, 096601 (2009).
 - [15] R. Dreyfus *et al.*, *Nature (London)* **437**, 862 (2005).
 - [16] F. Peruani and L. G. Morelli, *Phys. Rev. Lett.* **99**, 010602 (2007).
 - [17] A. Upadhyaya *et al.*, *Physica A (Amsterdam)* **293**, 549 (2001).
 - [18] L. Cisneros *et al.*, *Phys. Rev. E* **73**, 030901(R) (2006).
 - [19] H. Risken, *The Fokker-Planck Equation: Methods of Solution and Applications* (Springer, New York, 1989), 2nd ed., p. 32.
 - [20] V. Zaburdaev and H. Stark (to be published).
 - [21] P. E. Kloeden and E. Platen, *The Numerical Solution of Stochastic Differential Equations* (Springer, New York, 1999), p. 305.